Chemical Science International Journal

Volume 33, Issue 6, Page 225-240, 2024; Article no.CSIJ.127798
ISSN: 2456-706X
(Past name: American Chemical Science Journal, Past ISSN: 2249-0205)

Varied Analysis of Acid Dissociation Constants by Cyclic Voltammetry and UV-Visible to Determine the Aqueous Solubility of a New Diisopropylammonium Phenylsulfonate Molecule

Dame Seye [a,b*], Déthié Faye [c], Momath Lo [c*], Cheikh A. B. Diop [c], Mamadou Dieng [c], Cheikh A. K. Diop [b] and Modou Fall [c]

[a] Département Physique – Chimie, UFR Science et Technologie, Université Iba Der THIAM de Thiès, Sénégal.
[b] Laboratoire de Chimie Minérale et Analytique (LA.CH.MIA), Département de Chimie, Faculté des Sciences et Techniques, Université Cheikh Anta Diop, Dakar, Sénégal.
[c] Laboratoire de Chimie Physique Organique et d'Analyses Environnementales, Département de Chimie, Faculté des Sciences et Techniques, Université Cheikh Anta Diop, Dakar, Sénégal.

Authors' contributions

This work was carried out in collaboration among all authors. All authors read and approved the final manuscript.

Article Information

DOI: https://doi.org/10.9734/CSJI/2024/v33i6940

Open Peer Review History:
This journal follows the Advanced Open Peer Review policy. Identity of the Reviewers, Editor(s) and additional Reviewers, peer review comments, different versions of the manuscript, comments of the editors, etc are available here: https://www.sdiarticle5.com/review-history/127798

Original Research article

Received: 12/10/2024
Accepted: 14/12/2024
Published: 20/12/2024

**Corresponding author: E-mail: momath.lo@ucad.edu.sn, dame.seye@univ-thies.sn;*

Cite as: *Seye, Dame, Déthié Faye, Momath Lo, Cheikh A. B. Diop, Mamadou Dieng, Cheikh A. K. Diop, and Modou Fall. 2024. "Varied Analysis of Acid Dissociation Constants by Cyclic Voltammetry and UV-Visible to Determine the Aqueous Solubility of a New Diisopropylammonium Phenylsulfonate Molecule". Chemical Science International Journal 33 (6):225-40. https://doi.org/10.9734/CSJI/2024/v33i6940.*

ABSTRACT

The determination of dissociation constant, solubility and thermodynamic parameters are very important physico-chemical parameters in substances and their knowledge is of fundamental importance for the validation of a pharmaceutical ingredient target. The determination of these parameters for an agent candidate target diisopropylammonium phenylsulfonate (besylate) ($PhSO_3$-iPr_2NH_2) was determined by voltammetric and UV-visible methods.

The voltammetric method gave pKa1= 3.03±0.21 and pKa2= 10.23±0.59, while the UV-visible method determined two pKas values, pKa1= 2.21±0.04 and pKa2= 10.77±0.42 respectively. The thermodynamic parameter values calculated for the enthalpy (ΔH) and entropy (ΔS) of $PhSO_3$-iPr_2NH_2 are of the order of ΔH= 3429.96±82.30 $KJ.mol^{-1}$and ΔS = 11.85 ± 0.26 $KJ.mol^{-1}.K^{-1}$. These values suggest that the crystalline molecule is stable and the dissociation process is endothermic.

In addition, the Gibbs free energy of the molecule decreases with increasing temperature which confirmed the stability $PhSO_3$-iPr_2NH_2 crystalline. The solubility shows values between 1.3 and 70 mg/mL for pH values between 2.75 and 10.5 and reaches its maximum Smax = 70mg/mL at pH equals 2.75 and 10.5.

All these physico-chemical properties of $PhSO_3$-iPr_2NH_2, which are within the range of active pharmaceutical ingredients, could make it an excellent candidate of pharmaceutical ingredient. On the other hand, these results demonstrated the reliability and effectiveness of the voltammetric and UV-visible methods for the the determination of physico-chemical properties of molecules.

Keywords: Diisopropylammonium phenylsufonate; voltammetric method; UV-visible method; physicochemical parameters.

1. INTRODUCTION

The majority of drugs used in therapy have low water solubility, which can reduce bioavailability and the rate of dissolution [1]. So, because of their low solubility, drugs designed to be therapeutically active become a real danger to humans. Water solubility is a key parameter in drug formulation, as it has a major influence on the pharmacokinetics and pharmacodynamics of the drug [2]. In other words, the therapeutic efficacy of drugs administered orally or transdermally is highly depends on their water solubility. Water solubility enables the desired drug concentration to be reached in the systemic circulation, and obtained consequently optimal therapeutic response [3]. Based on Biopharmaceutical classification system (BCS) 35% to 40% of new (marketed) drugs suffer from poor water solubility which leads to low bioavailability, reduced therapeutic effects and dosage escalation [4]. On the other hand, 70% to 90% of drug candidates in development fail due to poor solubility and dissolution [5]. Thus, it becomes essential to find a way of increasing the dissociation rate and bioavailability of drugs [6,7]. The aim is to develop a less expensive, easier and faster technique for increasing the solubility of these drugs [8]. In this regard, the salification of medicines or the formation of medicinal salts is proving to be the safest and most reliable way of increasing solubility without unwanted side effects [9]. For example, the Enhancement of solubility and dissolution rate of dipyridamole a drug with low solubility was carried out by Yi et al. using salification method [10]. Gundlapalli et al. also used benzenesulfonic acid (BSA) as counterion with the objective of enhancing the solubility and dissolution of Suvorexant by salifying approach [11]. To form a drug salt, the free acid or base of the drug is combined with the base or acid of a potential counterion in specific molar ratios in a suitable solvent system. These latter participate in ionic interactions and crystallize under favorable conditions to give the solid salt [12-15]. Among potential counterions, phenylsulphonate-based salts, commonly known as besylate, are widely used as active pharmaceutical ingredients (APIs) in pharmaceutical development [16,17]. These salts help to improve aqueous solubility or increase the speed of dissolution thanks to their low toxicity potential and ease of synthesis [18]. It is in this context that we have witnessed a new era in the synthesis of besylate derivatives. For example, J. H. Seo et al [19] have developed a new technique for synthesising the besylate salt of cilostazol with the aim of improving the solubility of the drug cilostazol and its physico-chemical properties such as stability, bioavailability. All these substances have acidic or basic functional groups whose ionisation coefficients (pKa) affect their physico-chemical and biological properties. However, for the validation of any phenylsulphonate-derived counter-ion product, the determination of pKas values is a key parameter for the success of the salt to be formed [20,21]. As well as influencing the choice of counterion, it provides information on the stability of the product formed and the circulation of the drug in the organism.

To determine the acid dissociation constant values, several methods were used by the researchers, namely spectroscopy [22], electrophoresis [23], potentiometric titration [24] ,high-performance liquid chromatography (HPLC) and capillary electrophoresis (CE) [25]. UV-Visible spectrophotometry and cyclic voltammetry [26] are the most reliable methods for determining dissociation constants thanks to their accuracy and ease of use. They have advantages over other methods in that they are relatively simple and practical, requiring a small quantity of sample for accurate measurement and covering a wide range of pKa.

In the present work we have studied the thermodynamic parameters of a diisopropylammonium phenylsulphonate (besylate), a new crystalline molecule that we have recently synthesised for the first time [27]. This diisopropylammonium comes from diisopropylamine, a product recently used with dichloroacetate to inhibit the propagation and multiplication of liver cells [28]. The pKa values and thermodynamic parameters were determined in an aqueous medium. These parameters associated with solubility were determined by voltammetry and UV-visible method.

2. PRODUCTS, MATERIALS AND PROCEDURES

2.1 Products

Diisopropylammonium besylate ($PhSO_3$-iPr_2NH_2) with empirical formula ($C_{12}H_{21}NSO_3$) was synthesized by SEYE et al [**Error! Bookmark not defined.**]. Hydrochloric acid (HCl) and sodium dihydroxide (NaOH) were used as the titrating solution. Aqueous solutions used were prepared by an ultrapure Milli-Q (MQ 18.2 MΩχμ) water

2.2 Materials

Experiments were carried out using cyclic voltammetry and U-V Visible spectrophotometry. The pH meter and electronic balance were also used. Cyclic voltammetry allows us to visualize the oxidation and reduction current peaks of the $PhSO_3$-iPr_2NH_2 compound. It consists of a PSTRAS device linked to a cable with three electrodes (reference, counter and working electrode) immersed in a cell containing the solution, and another cable linked to a computer. The Thermos Fisher Scientific U-V Visible spectrophotometer, model G10S UV-Vis serial number 2L9U285217, plots absorbance as a function of wavelength. The pH/ mV/oC/oFmeter is a device for measuring the pH of a solution. It consists of an electronic box that displays the pH value and an electrode that measures this value.

2.3 Procedures

A three-electrode cell composed of a platinum working electrode (4 mm diameter), a platinum counter electrode and an Ag/AgCl reference electrode. The experiment was performed in the electrochemical cell containing 10mL of solution containing 5-10^{-2}M $PhSO_3$-iPr_2-NH_2 salt. Cyclic voltammetry measurements were then carried out after the addition of NaOH or HCl to vary pH values between 2-11 values.

All these curves were recorded using a cyclic voltammetry in the potential range between - 1 and 1.5 V/Ag/AgCl with a scan rate of 50mV/s.

UV-visible (UV-vis) absorption spectra of $PhSO_3$-iPr_2-NH_2 were recorded with a Thermo Fisher scientific UV-vis absorption spectrometer in 3mL of $PhSO_3$-iPr_2NH_2 of concentration 5.10^{-2} M. Experiments were repeated following the addition of titrating solution of NaOH (0.1M) and HCl (0.1M).

3. RESULTS AND DISCUSSION

3.1 Proton Transfer Mechanism of $PhSO_3$-iPr_2NH_2 Salt

Diisopropylammonium phenylsulfonate ($PhSO_3$-iPr_2NH_2) is a salt formed from a cation (or acidic site, diisopropylammonium) and an anion (or basic site, phenylsulfonate). The Scheme 1 represent the procedure for synthesis of $PhSO_3$-iPr_2NH_2 crystalline molecule and previously reported [**Error! Bookmark not defined.**]. $PhSO_3$-iPr_2NH_2 is capable of capturing or releasing a proton, depending on the nature of the medium. Diisopropylammonium phenylsulfonate behaves like an amphoteric, being able to combine with both acids and bases. Neutralization of the acidic site (diisopropylammonium) takes place in a basic medium in the presence of NaOH (schema 2), followed by the formation of water, while neutralization of the basic site (phenylsulfonate) takes place in an acidic medium in the presence of HCl (schema 3).

3.2 Study of the Behavior of PhS-iPr_2NH_2

3.2.1 By electrochemical methods

Fig. 1 shows cyclic voltammetry on the bare platinum electrode immersed in 10mL of 5.10^{-2} M $PhSO_3$-iPr_2NH_2 solution. Indeed, by cyclic voltammetry, the potential between - 1 and 1.5 V/Ag/AgCl at a scan rate of 50 mV/s, we observe the presence of two oxidation peaks and two reduction peaks corresponding to the redox behavior of the $PhSO_3$-iPr_2NH_2 crystalline molecule in solution on the working electrode.

Study of the voltammetric curve (Fig. 1) shows the presence of two anodic peaks at around 0.88 and -0.5 V/Ag/AgCl, and two reduction peaks at around -0.67 and 0.12 V/Ag/AgCl. The potentials of the oxidation peak at 0.88 V/Ag/AgCl and the reduction peak at 0.12 V/Ag/AgCl are very similar to those described for an aliphatic amine [29]. The presence of the second redox couple (-0.5 and - 0.67 V/Ag/AgCl) is linked to the presence of the phenylsulfonate group. These results show that the PhS-iPr_2NH_2 crystalline molecule is an electroactive compound in solution, exhibiting a reversible characteristic and confirming that it possesses two oxidizing/reducing couples.

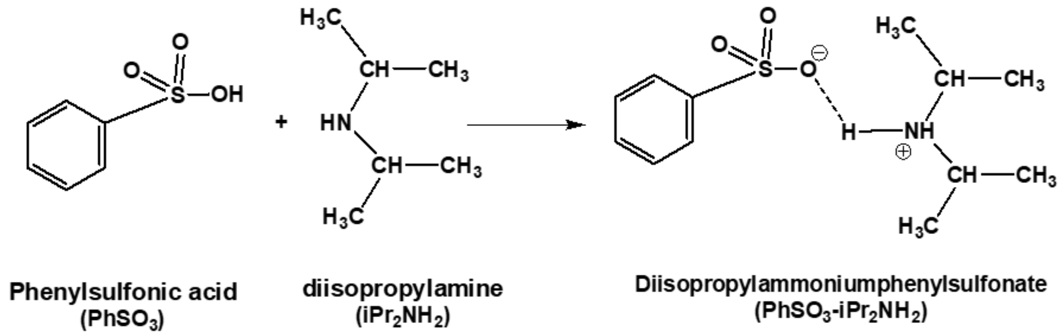

Schema 1. Procedure for synthesis of $PhSO_3$-iPr_2NH_2

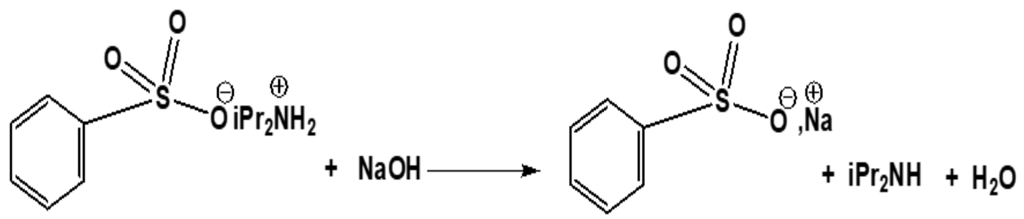

Schema 2. $PhSO_3$-iPr_2NH_2 reaction equation in a basic medium

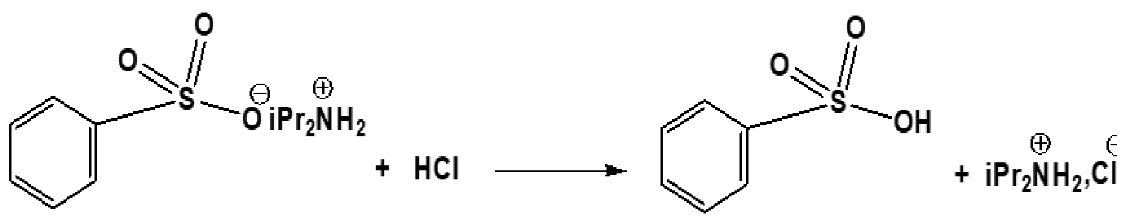

Schema 3. $PhSO_3$-iPr_2NH_2 reaction equation in acid medium

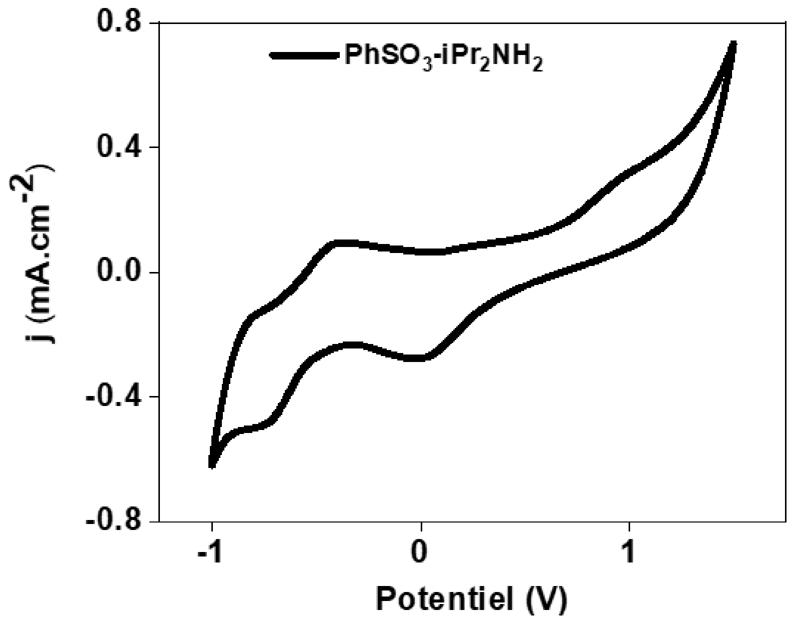

Fig. 1. Cyclic voltammetry curve for $PhSO_3$-iPr_2NH_2 (0.05M) in aqueous medium

3.2.2 By UV-Visible method

Fig. 2 shows the UV-visible spectrum of $PhSO_3$-iPr_2NH_2 salt in aqueous medium recorded between 200-500 nm. This figure shows a maximum absorption band around 300nm.

This absorption band is due to the л→л* electronic transitions of the phenyl group. These results show that the crystalline molecule possesses luminescence properties.

3.3 Process for the Determination of pKa Values

3.3.1 By electrochemical method

The results obtained previously illustrate that the compound $PhSO_3$-iPr_2NH_2 has two oxidizing/reducing pairs as mentioned above. For pKa determination by cyclic voltammetry, oxidation and reduction currents are measured as a function of solution pH after each addition of titrant solution. After each addition of a quantity of HCl or NaOH to the electrochemical cell containing 0.05 M $PhSO_3$-iPr_2NH_2, the pH of the solution is modified, accompanied by a more intense resulting current.

For an acid-base equilibrium $(AH \overset{K_a}{\rightarrow} A^- + H^+)$, the pKa is given by [30]:

$$K_a = \frac{[A^-][H^+]}{[AH]}$$

$$pK_a = pH - \log\left(\frac{[A^-]}{[HA]}\right)$$

With [AH] and $[A^-]$ the respective concentrations of the acid and its conjugate base. The resulting total current is $I = I_{A^-}[A^-] + I_{AH}[AH]$.

This is a method for determining pKa based on anodic (I_{AH}) and cathodic (I_{A^-}) currents by applying the equation. After combining all these data, we obtain Eq1:

$$pKa = pH - \log\left(\frac{I_{AH} - I_{A^-}}{I - I_{A^-}} - 1\right) \quad \text{(Eq1) [31]}$$

3.3.1.1 Effect of HCl acid addition

Fig. 3 shows voltammograms of the response of the 0.05 M solution of PhS-$O_3iPr_2NH_2$ in aqueous medium in the absence and presence of added HCl (0.1M). It can be seen that the addition of HCl to $PhSO_3$-iPr_2NH_2 leads to an increase in the oxidation peak and the reduction peak characteristic of the $C_6H_5SO_3H/C_6H_5SO_3$- couple (schema 2). Fig. 3a shows that, as a function of the progressive addition of HCl, the oxidation peak at -0.5 V/Ag/AgCl shifts towards positive potentials, while the reduction peak at -0.67 V/Ag/AgCl tends towards negative potentials. These results show that the reaction between $PhSO_3$-iPr_2NH_2 and H+ increases the charge density of the molecule [32]. In addition, the basic site of $PhSO_3$-iPr_2NH_2 undergoes neutralization, resulting in a decrease in the pH value, which tends towards acidic pH values. On the other hand, the redox couple at around 0.88 and 0.12 V/Ag/AgCl remains unchanged, suggesting that the $PhSO_3$-iPr_2NH_2 molecule is in acid-base salt form, and could be confirmed by the same technique, this time with the addition of a titrating NaOH solution.

3.3.1.2 Effect of NaOH base addition

The acid-base behavior of the $PhSO_3$-iPr_2NH_2 crystalline molecule was studied by adding a NaOH (0.1M) titrating solution. For this purpose, various measurements were recorded in an aqueous solution of 0.05 M $PhSO_3$-iPr_2NH_2 after each addition of a quantity of NaOH titrating solution and represented in Fig. 3b. These curves show a progressive increase in the intensity of the oxidation peaks as a function of the volume of NaOH added. Fig. 3b reveals that the oxidation peak at around 0.88 V/Ag/AgCl shifts towards positive potentials, while that at -0.5 V/Ag/AgCl remains practically unchanged.

These results confirm those previously described and indicate that the strong base NaOH attacks the acid site (Scheme 1). The addition of NaOH in solution in the presence of the $PhSO_3$-iPr_2NH_2 crystalline molecule enhances the electrochemical properties, leading to an increase in the charge density and consequently the conductivity of the medium. Electron donors can generate a high charge density. In basic media, an improvement in the rate of charge transfer is noted, leading to an increase in current intensity [33]. Furthermore, the reduction peak disappeared at around -0.67V/Ag/AgCl in the presence of NaOH. These results indicate that the presence of NaOH in the electrolyte medium blocks the reduction process of the $PhSO_3$-iPr_2NH_2 compound in solution.

3.3.2 UV-visible spectroscopy

UV-Visible spectrophotometry provides information on the excitation wavelength of compounds, and on the difference in chemical structure between compounds. To determine the acid dissociation constant pKa of a molecule accurately and reliably, UV-visible spectrophotometry is unquestionably the method of choice, especially if the substance is too insoluble. In this method, the pKa depends on the ionized forms of the molecule and the pH. The extent of a compound's ionization plays a fundamental role in characterizing its absorption, distribution, metabolism and excretion (ADME) profile [34,35].

Two methods are used to determine pKa values:

First method: This is a graphical method, plotting the pH curve as a function of $\log(A_m/A_i)$.

If $\log(A_m/A_i)$ =0, the corresponding pH value is equal to the pKa value.

Second method: this is a direct method, depending on the nature of the ionized and non-ionized forms of the compound at different pH values. It provides information on the accuracy of the first method by applying the equation below (Eq. 2).

In UV-Visible spectrophotometry, the pKa value is given by the following equation:

$$\mathrm{pKa} = \mathrm{pH} + \log\frac{A_m - A}{A - A_i} \quad \text{(Eq 2)}$$

A absorbance des espèces intermédiaires

A_m absorbance de l'espèce moléculaire

A_i absorbance l'espèce ionisée

pH représente la valeur du pH du milieu intermédiaire [36,37].

For this method, the pKa value depends on the absorbance of the ionized forms, hence the need to ionize the molecule by adding acid or base.

3.3.2.1 Effect of NaOH addition

Figs. 4a, 4b and 4c show the UV-visible spectra of $PhSO_3$-iPr_2NH_2 in solution as a function of the amount of NaOH added. It can be seen that the addition of NaOH (0 – 800 µL) to the $PhSO_3$-iPr_2NH_2 solution first leads to a decrease in the intensity of the absorption band around 300 nm (Fig. 4a). This decrease is due to the interactions of the OH- base with the proton of the cationic function of $PhSO_3$-iPr_2NH_2 (-O----H-), which leads to the progressive formation of the conjugated base in solution. This results in a decrease in the concentration of the cationic function, leading to a drop in absorption intensity. The latter, responsible for absorption emission at the same wavelength, increasingly loses its supremacy, leading to a hypochromic effect.

These results correlate with those developed by A. Garcia-Leis in the case of the UV-visible study of the compound 2,2'-azino-bis (3-ethylbenzothiazoline-6-sulfonic acid (ABTS) [38].

Secondly, there is an increase in absorption intensity at the same wavelength as before, from 800 µL up to 1300 µL of added NaOH (Fig. 4b). In this case, the hyperchromic effect is observed, showing that at 800 µL the conjugated base becomes the majority in solution and substitutes the cationic function in the absorption emission. And finally, with NaOH volumes above 1300 µL (Fig. 4c), a decrease in absorption intensities is again noted.

These results show that the entire cationic part of $PhSO_3$-iPr_2NH_2 is completely neutralized and the concentration of the conjugated base responsible for the absorption band decreases with dilution.

3.3.2.2 Effect of HCl acid addition

The UV-visible spectra of the $PhSO_3$-iPr_2NH_2 crystalline molecule in solution as a function of the volume of HCl (0-5000 µL) added are shown in Fig. 5. As a function of the amount of HCl added, the absorbance band around 300nm decreases considerably, reflecting the attachment of the H^+ proton to the O^- of the phenylsulfonate function, resulting in an interaction (-O-H-) and the formation of the conjugate acid of the $PhSO_3$-iPr_2NH_2 anion function. Moreover, these interactions lead to protonation of the anionic part of $PhSO_3$-iPr_2NH_2, followed by a reduction in the strength of the latter in solution, the concentration of which is proportional to absorption.

These results point to a hypochromic effect due to the action of HCl on $PhSO_3$-iPr_2NH_2 in solution [**Error! Bookmark not defined.**].

3.4 Calculation of pKa Values

3.4.1 By electrochemical methods

Fig. 6a shows the variation of anodic currents as a function of pH in acidic medium. It provides information on the range of pKa values in the region where current intensity tends towards the maximum value [39]. In this case, the ($C_6H_5SO_3H/C_6H_5SO_3^-$) couple is brought into play by the amount of acid added, and is accompanied by an increase in the anodic and cathodic currents. This increase is linked to the degree of interaction of the hydrogen bond [40]. In addition, the curve shows a vertical tangent inflection between 2.9 and 3.1, corresponding to neutralization of the anionic part of the PhS-iPr_2NH_2 crystalline molecule in solution. These results correlate with those found by J. Zhao [41] for cyclic voltammetry titration. Applying the formula linking pKa to pH and currents, anodic and cathodic (Eq1), we find a pKa value of the order of 3.03±0.21. The Fig. 6b corresponding to the variation of anodic currents as a function of pH in basic medium shows a curve with the appearance of a classic weak acid-strong base assay, and a significant pH jump between 10.4 - 11.2. It provides information on the pKa value page, which lies in the pH range where the anode current approaches its maximum value. The data allow us to determine the pKa value by applying equation 2, and we find a value of pKa2= 10.23±0.59.

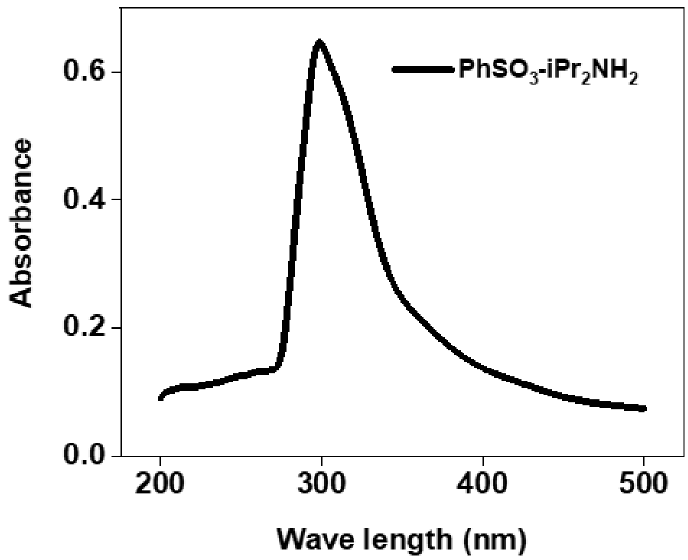

Fig. 2. UV-visible curve of $PhSO_3$-iPr_2NH_2 salt (0.05M) in aqueous medium

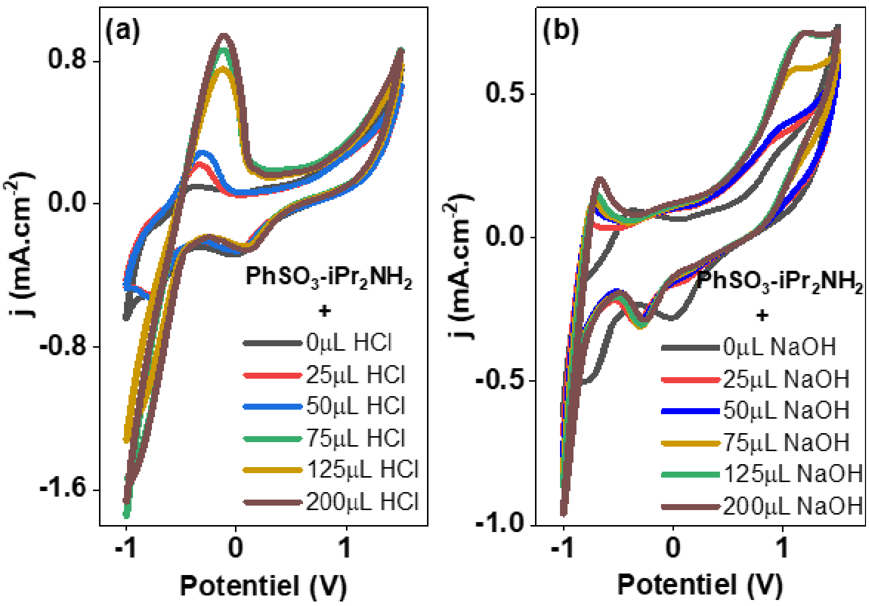

Fig. 3. Voltammetric curves for $PhSO_3$-iPr_2NH_2 salt in aqueous medium in the absence and presence of (a) HCl (b) NaOH

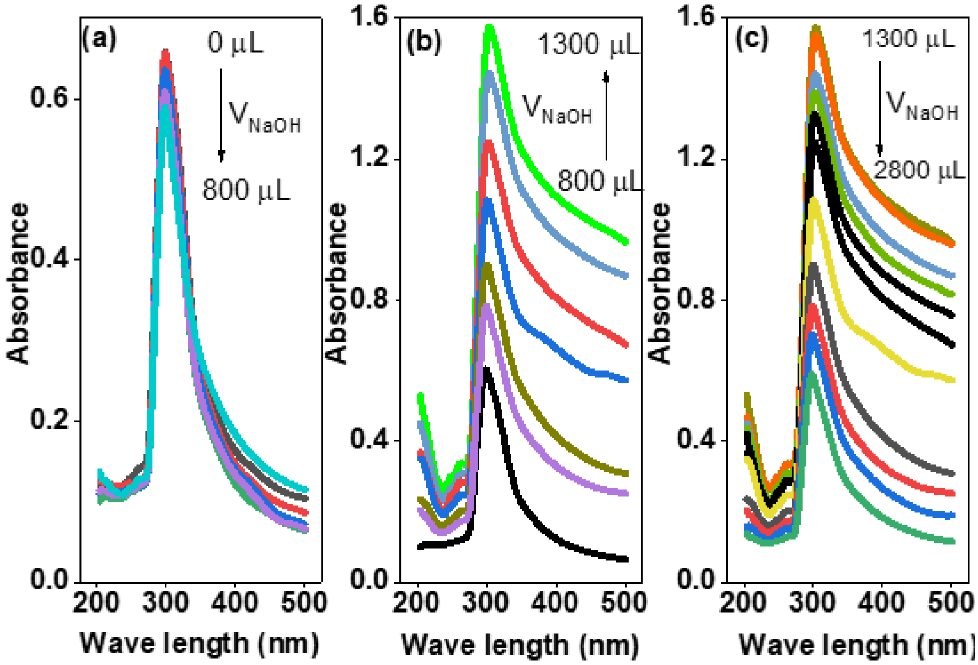

Fig. 4. Superposition curves of UV-visible spectra of $PhSO_3$-iPr_2NH_2 at different NaOH volumes (a) range from 0 to 800 µL (b) range from 800 to 1300 µL and (c) range from 1300 to 2800 µL

3.4.2 UV-visible analysis

To confirm the pKas values found electrochemically, the UV-visible analysis technique is commonly used. For the determination of pKas values using the first method, pH curves as a function of log(Am/Ai) are often exploited (Figs. 7a and 7b). In Fig. 7a, the decimal logarithm of the absorbance ratio of the molecular form to the ionized form increases with pH. Graphically, the value pKa_2=11.03 is found for $C_6H_{14}NH_2^+/C_6H_{14}NH$, corresponding to pH = pKa under conditions where $\log(A_m/A_i) = 0$. The second method (Eq2), whose data gives a value of pKa_2=10.77±0.42. Fig. 7b, on the other hand, shows the pKa value for the

($C_6H_5SO_3H/C_6H_5SO_3^-$) couple. Applying the first method corresponding to the variation of pH as a function of log(Am/Ai) gives a pKa_1 value of the order of 2.4 in the case where $\log(A_m/A_i) = 0$. The second method (Eq2) gives a pKa1 value of 2.21±0.04. These pKa values found by the two methods give a difference of around 0.3, confirming the reliability of the UV-visible technique.

3.5 Determination of Thermodynamic Parameters

Calculation of thermodynamic parameters: ΔG, ΔH and ΔS

Thermodynamic parameters are important in molecular chemistry. For the determination of these parameters, the Vant'Hoff equation is the most used (Eq 3).

$$\frac{d\ln Ka}{dT} = \frac{\Delta H}{RT^2} \qquad \text{(Eq 3)}$$

ΔH molar enthalpy,

R universal gas constant and is equal to 8.314 $J.mol^{-1}.K^{-1}$

T temperature in Kelvin (K).

The Gibbs free energy ΔG is also linked to the reaction constant by the relation (Eq 4):

$$\Delta G = -RT\ln Ka \qquad \text{(Eq 4)}$$

It is possible to determine the Gibbs free energy from the absorbance value obtained by UV-visible spectroscopy by applying the following relationship (Eq 5):

$$\Delta G = -2.303RT\log(A) \qquad \text{(Eq 5)}$$

With A is the absorbance value [42].

The results obtained from equation 5 are shown in Table 1.

The relationship between the Gibbs free energy ΔG, the entropy ΔS and the enthalpy ΔH is given by the third law of thermodynamics (Eq 6):

$$\Delta G = \Delta H - T\Delta S \qquad \text{(Eq 6)}$$ [43].

Eq 6 makes it possible to deduce the values of ΔS and ΔH by plotting the curve ΔG as a function of the temperature T (Fig. 8). The intercept coincides with the value of ΔH and the slope corresponds to the opposite of ΔS.

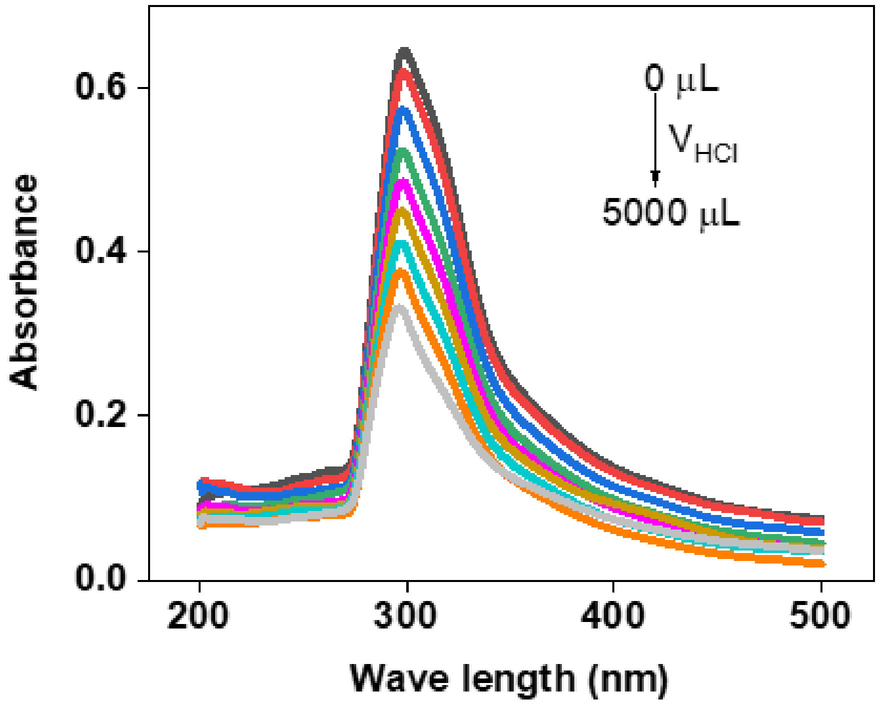

Fig. 5. UV-visible curve of $PhSO_3$-iPr_2NH_2 (0.05M) salt with HCl (0.1N) 0 - 5000 µL

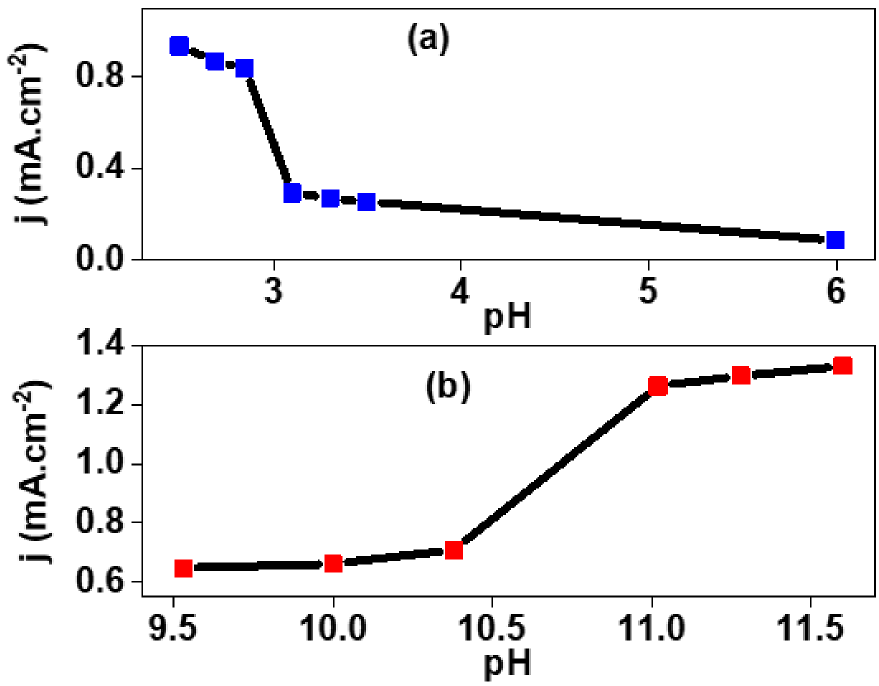

Fig. 6. Current density curve as a function of pH in (a) acidic medium and (b) basic medium

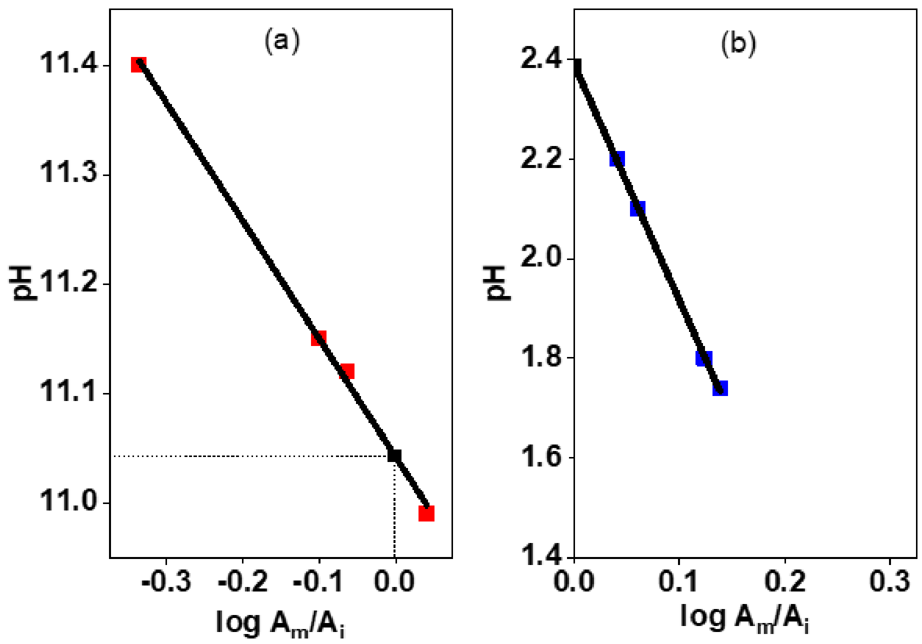

Fig. 7. pH vs. log(A_m/A_i) curve (a) in basic medium and (b) in acidic medium.

Table 1. Value of absorbances and ΔG as a function of temperature

Température T (K)	298	303	308	313	318	323
Absorbance	0,890	0,970	1,090	1,112	1,135	1,160
ΔG(KJ.mol^{-1})	288,738	76,745	-220,716	-276,308	-334,858	-398,642

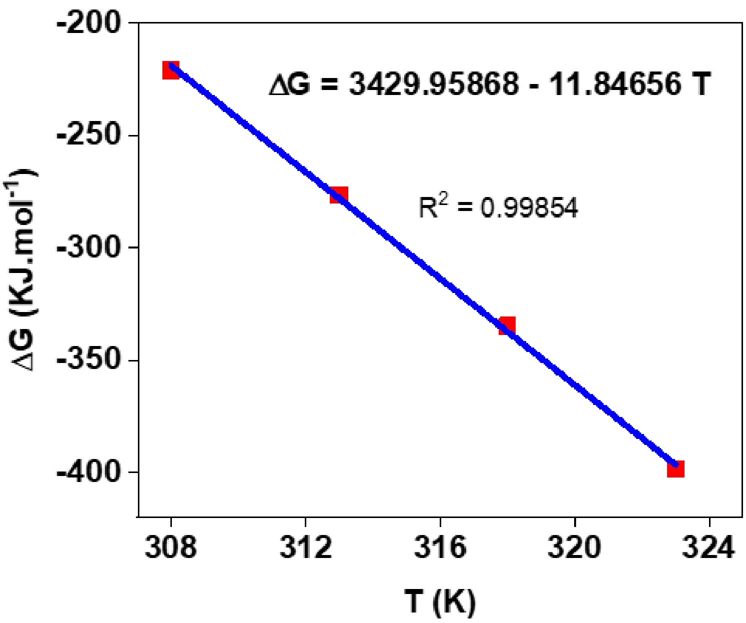

Fig. 8. Variation curve of ΔG as a function of temperature T

Table 2. The different values of ΔG, ΔH and ΔS for the PhS-iPr$_2$NH$_2$ crystalline molecule in solution

Température (K)	ΔG(KJ.mol^{-1})	ΔH(KJ.mol^{-1})	ΔS(J.mol^{-1}.K^{-1})
298	288.74±11.43		
303	76.75±2.99		
308	-220.72±8.48	3429,96 ± 82,30	11,85 ± 0.26
313	-276.31±10.45		
318	-334.86±12.46		
323	-398.64±11.84		

The obtained values of standard enthalpy, entropy and Gibbs free energy of the dissociation of PhSO$_3$-iPr$_2$NH$_2$ are given in Table 2. It seems that the values of ΔG decrease with increasing temperature. These results are similar to those of Li [44], which justifies that the dissociation process of PhSO$_3$-iPr$_2$NH$_2$ increases with increasing temperature. The positive value of ΔH= 3429.96 kJ.mol^{-1} indicates that the dissociation is endothermic [45]. The positive values of ΔG indicate that the dissociation process is not spontaneous for the temperature between 298 and 303 K. The decreases of ΔG as a function of temperature showed that the dissociation of the PhSO$_3$-iPr$_2$NH$_2$ crystalline molecule is favored by the increase in temperature. However, the value of ΔS = 11.85 ± 0.26 J.mol^{-1}.K^{-1} due to increased disorder resulting from dissociation processes. All these thermodynamic parameters of PhSO$_3$-iPr$_2$NH$_2$ confirm the stability of the crystalline molecule in an aqueous medium.

3.6 Determination of Solubility

For the determination of the solubility of diisopropylammonium phenylsulfonate, an amphoric compound composed of a monoacid diisopropylammonium and a monobase phenylsulfonate, the Henderson-Hasselbalch (HH) equation was used [46]

For a monoacid: The HH equation for a monoacid is given by Eq 7:

$$S = S_0(10^{pH-pKa} + 1) \qquad \text{(Eq 7) [47]}$$

Fig. 9a shows the solubility of the $C_6H_{14}NH_2^+$ cation as a function of pH. We see that the free cationic form has a value of S_{max} = 33.5 mg/mL with an intrinsic solubility value S_0 =1.3 mg/mL.

For a salt: the HH equation for a salt composed of acid and base is given by Eq 8:

$$\log S = \log S_0 + \log(10^{pKa1-pH} + 10^{pH-pKa2} + 1) \quad \text{(Eq 8) [48]}$$

Fig. 9b shows the variation in solubility as a function of pH of PhS-iPr_2NH_2, an amphoteric compound. For this amphoteric the variation in pH leads to an exponential increase in solubility with an S_{max} value approximately equal to 70 mg/mL double the solubility of the salt forms of the free acid. These results show that the presence of the besylate anion increases the solubility of diisopropylammonium to a value practically equal to twice the maximum solubility of the cation alone. This once again shows the importance of the besylate anion in improving the solubility of pharmaceutical compounds. Furthermore, the salt of diisopropylammonium besylate or (diisopropylammonium phenylsufonate) has an aqueous solubility of approximately 70 mg/Ml which greater than that of several drug candidates approved by the Administration of Medication Food (ANM) [49] Table 3 shows a comparative study of the solubility of diisopropylammonium besylate with other drugs.

This study demonstrates that diispropylammonium besylate solubility is excellent is excellent compared to the solubility values of other molecules, and therefore could be considered as a potential API in the design of pharmaceutical salts.

Table 3. Comparative study of the solubility of diisopropylammonium besylate with other drugs

Molecules	MW	pKa	Solubility (mg/mL)	Ref
Amlodipine besylate	409	9.0	2.22	[50]
Bepotastine besylate	389	4.4 ; 8.9	23.3	[50]
Camostat mesylate	398	9.1	45.5	[51]
Haloperidol phosphate	471	8.3	3.4	[51]
Ethionamide maleate	280	-	19.9	[52]
Diisopropylammonium besylate	259	2.2 ; 10.8	70	This work

MW_ Molecular weight; Ref references

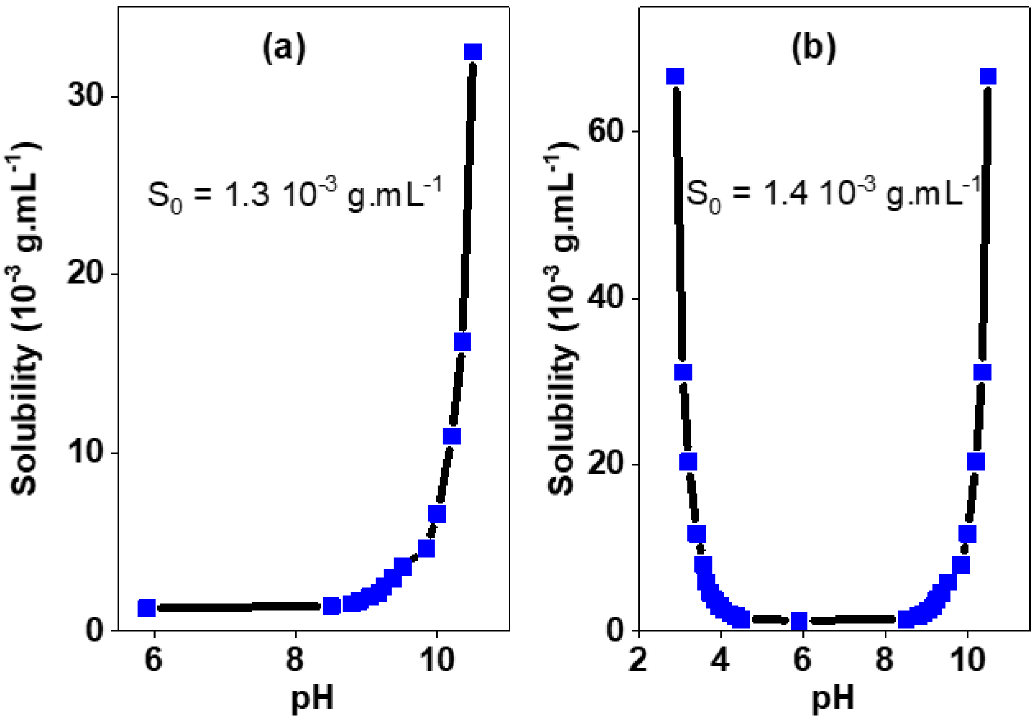

Fig. 9. pH-solubility curve (a) of the diisopropylammonium cation $C_6H_{14}NH_2^+$ (b) of $PhSO_3$-iPr_2NH_2

4. CONCLUSION

Knowledge of the characteristics of an API is an important parameter for the design of a pharmaceutical salt meeting the standard required by the World Health Organization (WHO). Our work consists of studying the physicochemical parameters of diisopropylammonium phenylsulfonate, a potential API which could be used as a counterion for the formation of pharmaceutical salts. In our previous experiments, it has been demonstrated that diisopropylammonium phenylsulfonate behaves like an amphoteric because it is capable of capturing a proton in an acidic medium and giving it up in a basic medium. In addition, the cyclic voltammetry curve confirmed that PhS-iPr_2NH_2 had two acid-base pairs: sulfonic acid/phenylsulfonate $C_6H_5SO_3H$/ $C_6H_5SO_3^-$ and diisopropylammonium/ diisopropylamine $C_6H_{14}NH_2^+$/$C_6H_{14}NH$. The thermodynamic parameters of $PhSO_3$-iPr_2NH_2 and the pKas values were determined by cyclic voltammetry and UV-visible. These two methods made it possible to obtain the pKa values of the two couples with a few errors. These methods also allowed us to calculate the solubility value of the molecule which is much higher than that developed in the literature and accepted as an active pharmaceutical ingredient.

The physicochemical parameters obtained are in the range of APIs and are satisfactory for the use of $PhSO_3$-iPr_2NH_2 as a counterion for the synthesis of pharmaceutical salts. The $PhSO_3$-iPr_2NH_2 crystalline molecule could be a potential API candidate with the aim of improving the solubility, efficacy, bioavailability and safety of drug molecules.

DISCLAIMER (ARTIFICIAL INTELLIGENCE)

Authors declare that no generative AI technologies such as large language models (chatgpt, copilot, etc.) and text-to-image generators have been used during the writing or editing of this manuscript.

COMPETING INTERESTS

Authors have declared that no competing interests exist.

REFERENCES

1. Bhalani DV, Nutan B, Kumar A, Singh Chandel AK. Bioavailability enhancement techniques for poorly aqueous soluble drugs and therapeutics. Biomedicines. 2022;10(9):2055.
Available:https://doi.org/10.3390/biomedicines10092055
2. Liu X, Zhao L, Wu B, Chen F. (Improving solubility of poorly water-soluble drugs by protein-based strategy: A review. International Journal of Pharmaceutics. 2023;634:122704.
3. Coltescu AR, Butnariu M, Sarac I. The importance of solubility for new drug molecules. Biomedical and Pharmacology Journal. 2020;13(2):577-583.
Available:https://dx.doi.org/10.13005/bpj/1920
4. Khan KU, Minhas MU, Badshah SF, Suhail M, Ahmad A, Ijaz S. Overview of nanoparticulate strategies for solubility enhancement of poorly soluble drugs. Life Sciences. 2022;291:120301.
Available:https://doi.org/10.1016/j.lfs.2022.120301
5. Jouyban A, Rahimpour E. Karimzadeh, Z. A new correlative model to simulate the solubility of drugs in mono-solvent systems at various temperatures. Journal of Molecular Liquids. 2021;343:117587.
Available:https://doi.org/10.1016/j.molliq.2021.117587
6. Mannava MC, Dandela R, Tothadi S, Solomon KA, Nangia, AK. (2020). Naftopidil molecular salts with improved dissolution and permeation. Crystal Growth & Design. 2020;20(5):3064-3076.
Available:https://doi.org/10.1021/acs.cgd.9b01689
7. Banerjee R, Bhatt PM, Ravindra NV, Desiraju GR. Saccharin salts of active pharmaceutical ingredients, their crystal structures, and increased water solubilities. Crystal Growth & Design. 2005;5(6):2299-2309.
Available:https://doi.org/10.1021/cg050125l
8. Yang D, Cao J, Jiao L, Yang S, Zhang L, Lu Y, Du G. Solubility and stability advantages of a new cocrystal of berberine chloride with fumaric acid. ACS Omega. 2020;5(14):8283-8292.
Available:https://doi.org/10.1021/acsomega.0c00692
9. Yi D, Dong Y, Yao Y, Hong M, Zhu B, Ren GB, Qi MH. (Enhancement of solubility and dissolution rate of dipyridamole by salifying: Preparation, characterization, and theoretical calculation. Journal of Molecular Structure. 2024;1296:136838.

10. Yi D, Dong Y, Yao Y, Hong M, Zhu B, Ren GB, Qi MH. Enhancement of solubility and dissolution rate of dipyridamole by salifying: Preparation, characterization, and theoretical calculation. Journal of Molecular Structure. 2024;1296:136838.
11. Gundlapalli S, Devarapalli R, Mudda RR, Chennuru R, Rupakula R. Novel solid forms of insomnia drug suvorexant with improved solubility and dissolution: accessing salts from a salt solvate route. CrystEngComm. 2021;23(44):7739-7749.
12. Thackaberry EA. Non-clinical toxicological considerations for pharmaceutical salt selection. Expert Opinion on Drug Metabolism & Toxicology. 2012;8(11):1419-1433.
Available:https://doi.org/10.1517/17425255.2012.717614
13. Aungst BJ. Optimizing oral bioavailability in drug discovery: An overview of design and testing strategies and formulation options. Journal of Pharmaceutical Sciences. 2017;106(4):921-929.
Available:https://doi.org/10.1016/j.xphs.2016.12.002
14. Saal C, Becker A. Pharmaceutical salts: A summary on doses of salt formers from the Orange Book. European Journal of Pharmaceutical Sciences. 2013;49(4):614-623.
Available:https://doi.org/10.1016/j.ejps.2013.05.026
15. Skořepová E, Bím D, Husak M, Klimes J, Chatziadi A, Ridvan L, al. Increase in solubility of poorly-ionizable pharmaceuticals by salt formation: A case of agomelatine sulfonates. Crystal Growth & Design. 2017;17(10):5283-5294.
Available:https://doi.org/10.1021/acs.cgd.7b00805
16. Bharate SS. Recent developments in pharmaceutical salts: FDA approvals from 2015 to 2019. Drug Discovery Today. 2021; 26(2):384-398.
17. Muleva CT, Bharate SS. Halide counterions in FDA-approved pharmaceutical salts. Journal of Drug Delivery Science and Technology. 2023;104999.
18. Hajikarimian Y, Yeo S, Ryan RW, Levett P, Stoneley C, Singh P. Investigation into the formation of the genotoxic impurity ethyl besylate in the final step manufacturing process of UK-369,003-26, a novel PDE5 inhibitor. Organic Process Research & Development. 2010;14(4):1027-1031.
Available:https://doi.org/10.1021/op100141g
19. Seo JH, Park JB, Choi WK, Park S, Sung YJ, Oh E, al. Improved oral absorption of cilostazol via sulfonate salt formation with mesylate and besylate. Drug design, Development and Therapy. 2015;3961-3968.
Available:https://doi.org/10.2147/DDDT.S87687
20. Bharate SS. Carboxylic acid counterions in FDA-approved pharmaceutical salts. Pharmaceutical Research. 2021;38:1307-1326.
Available: https://doi.org/10.1007/s11095-021-03080-2
21. Nyamba I, Sombie CB, Yabre M, Zime-Diawara H, Yameogo J, Ouedraogo S, & al. Pharmaceutical approaches for enhancing solubility and oral bioavailability of poorly soluble drugs. European Journal of Pharmaceutics and Biopharmaceutics. 2024;114513.
22. Qiu J, Yu L, Kirsch LE. Estimated pKa values for specific amino acid residues in daptomycin. Journal of Pharmaceutical Sciences. 2011;100(10):4225-4233.
Available:https://doi.org/10.1002/jps.22608
23. Konášová R, Dytrtová JJ, Kašička V. Determination of acid dissociation constants of triazole fungicides by pressure assisted capillary electrophoresis. Journal of Chromatography A. 2015;1408: 243-249.
Available:https://doi.org/10.1016/j.chroma.2015.07.005
24. Meloun M, Ferenčíková Z, Málková H, Pekárek T. Thermodynamic dissociation constants of risedronate using spectrophotometric and potentiometric pH-titration. Central European Journal of Chemistry. 2012;10, 338-353.
Available:https://doi.org/10.2478/s11532-011-0150-3
25. Ke J, Dou H, Zhang X, Uhagaze DS, Ding X, Dong Y. Determination of pKa values of alendronate sodium in aqueous solution by piecewise linear regression based on acid-base potentiometric titration. Journal of Pharmaceutical Analysis. 2016;6(6):404-409.
Available:https://doi.org/10.1016/j.jpha.2016.07.001
26. Rivas-Sánchez AK., Guzmán-Hernández DS, Ramírez-Silva MT, Romero-Romo M, Palomar-Pardavé, M. Quinizarin characterization and quantification in aqueous media using UV-VIS

spectrophotometry and cyclic voltammetry. Dyes and Pigments. 2021;184:108641. Available:https://doi.org/10.1016/j.dyepig.2020.108641

27. Seye D, Diop CAK, Diop L, Geiger DK. Diisopropylammonium benzenesulfonate. IUCrData. 2018;3(6):x180876.
28. Yan C, Wu XY, Luo OY, Su L, Ding YT, Jiang Y, Yu DC. Diisopropylamine dichloroacetate alleviates liver fibrosis through inhibiting activation and proliferation of hepatic stellate cells. Int J Clin Exp Med. 2019;12(4):3440-8.
29. Adenier A, Chehimi MM, Gallardo I, Pinson J, Vilà N. Electrochemical oxidation of aliphatic amines and their attachment to carbon and metal surfaces. Langmuir. 2004;20(19) 8243–8253.
30. Mishra SP, Pandey VK, Yadav AS, Singh RP. pH Determination of Acetic Acid-Sodium Acetate Buffer: An Application of Henderson-Hasselbalch Equation at Room Temperature. Chemical Science International Journal. 2024;33(6):32-38.
31. Gooding JJ, Hale PS, Maddox LM, Shapter JG. Surface pKa of self-assembled monolayers. Journal of Chemical Education. 2005;82(5):779. Available:https://doi.org/10.1021/ed082p779
32. Pang J, Dou Z, Lin M, Xu W, Zhai S, Han Y, Wang J. Mechanism of voltammetric determination of pKa of Brønsted–Lowry acids in aprotic solvent by quinone reduction. Microchemical Journal. 2010; 152:104324. Available:https://doi.org/10.1016/j.microc.2019.104324
33. Mattioli IA, Baccarin M, Cervini P, Cavalheiro ET. Electrochemical investigation of a graphite-polyurethane composite electrode modified with electrodeposited gold nanoparticles in the voltammetric determination of tryptophan. Journal of Electroanalytical Chemistry. 2019;835:212-219. Available:https://doi.org/10.1016/j.jelechem.2018.12.056
34. Pandey MM, Jaipal A, Kumar A, Malik R, Charde SY. Determination of pKa of felodipine using UV–Visible spectroscopy. Spectrochimica Acta Part A: Molecular and Biomolecular Spectroscopy. 2013;115:887-890. Available:https://doi.org/10.1016/j.saa.2013.07.001
35. Völgyi G, Ruiz R, Box K, Comer J, Bosch E, Takács-Novák K. Potentiometric and spectrophotometric pKa determination of water-insoluble compounds: validation study in a new cosolvent system. Analytica Chimica Acta. 2007;583(2):418-428. Available:https://doi.org/10.1016/j.aca.2006.10.015
36. Dubey SK, Singhvi G, Tyagi A, Agarwal H, Krishna KV. Spectrophotometric determination of pKa and Log P of risperidone. Journal of Applied Pharmaceutical Science. 2017;7(11):155-158.
37. Silva FV, Resende S, Araújo AN, Prior JA. Determination of pKa (s) of nilutamide through UV-visible spectroscopy. Microchemical Journal. 2018;138 :303-308. Available:https://doi.org/10.1016/j.microc.2018.01.025
38. Garcia-Leis A, Jancura D, Antalik M, García-Ramos JV, Sánchez-Cortés S, Jurasekova Z. Catalytic effects of silver plasmonic nanoparticles on the redox reaction leading to ABTS+ formation studied using UV-visible and Raman spectroscopy. Physical Chemistry Chemical Physics. 2016;18(38):26562-26571. Available:https://doi.org/10.1039/C6CP04387A
39. Joo J, Uchida T, Cuesta A, Koper MT, Osawa M. Importance of acid–base equilibrium in electrocatalytic oxidation of formic acid on platinum. Journal of the American Chemical Society. 2013;135(27): 9991-9994. Available:https://doi.org/10.1021/ja403578s
40. Gupta N, Linschitz H. Hydrogen-bonding and protonation effects in electrochemistry of quinones in aprotic solvents. Journal of the American Chemical Society. 1997;119 (27):6384-6391. Available:https://doi.org/10.1021/ja970028j
41. Zhao J, Luo L, Yang X, Wang E, Dong S. Determination of surface pKa of SAM using an electrochemical titration method. Electroanalysis: An International Journal Devoted to Fundamental and Practical Aspects of Electroanalysis. 1999;11(15): 1108-1113.
42. Inwati GK, Kumar P, Roos WD, Swart HC, Singh M. UV-irradiation effects on tuning LSPR of Cu/Ag nanoclusters in ion exchanged glass matrix and its thermodynamic behaviour. Journal of Alloys and Compounds. 2020;823: 153820.

Available:https://doi.org/10.1016/j.jallcom.2020.153820

43. Lima EC, Hosseini-Bandegharaei A, Moreno-Piraján JC, Anastopoulos I. A critical review of the estimation of the thermodynamic parameters on adsorption equilibria. Wrong use of equilibrium constant in the Van't Hoof equation for calculation of thermodynamic parameters of adsorption. Journal of Molecular Liquids. 2019;273:425-434.
Available:https://doi.org/10.1016/j.molliq.2018.10.048
44. Li L, Hsu TY. Gibbs free energy evaluation of the fcc (γ) and hcp (ε) phases in Fe-Mn-Si alloys. Calphad. 1997;21(3):443-448.
Available:https://doi.org/10.1016/S0364-5916(97)00044-8
45. Ayyildiz Y, Tarhan L. Problem-based learning in teaching chemistry: Enthalpy changes in systems. Research in Science & Technological Education. 2018;36(1):35-54.
Available:https://doi.org/10.1080/02635143.2017.1366898
46. Sugano K, Okazaki A, Sugimoto S, Tavornvipas S, Omura A, Mano T. Solubility and dissolution profile assessment in drug discovery. Drug Metabolism and Pharmacokinetics. 2007; 22(4):225-254.
Available:https://doi.org/10.2133/dmpk.22.225
47. Bala I., Bhardwaj V, Hariharan S, Kumar MR. Analytical methods for assay of ellagic acid and its solubility studies. Journal of Pharmaceutical and Biomedical Analysis. 2016;40(1):206-210.
Available:https://doi.org/10.1016/j.jpba.2005.07.006
48. Lo M, Faye D, Seye D, Dieng M, Sall ML, Thiaré DD, Abdou KD. Diaw Fall M. A novel method for combination of ionic conductivity and ph-metry methods for the determination of the aqueous solubility of a new diisopropylammonium hydrogenmaleate crystalline molecule. International Research Journal of Pure and Applied Chemistry. 2024;25(6): 12-27.
Available:https://doi.org/10.9734/irjpac/2024/v25i6882.
49. De Melo CC, da Silva CC, Pereira CC, Rosa PC, Ellena J. Mechanochemistry applied to reformulation and scale-up production of Ethionamide: Salt selection and solubility enhancement. European Journal of Pharmaceutical Sciences. 2016;81:149-156.
Available:https://doi.org/10.1016/j.ejps.2015.10.007
50. Ono A, Tomono T, Ogihara T, Terada K, Sugano K. Investigation of biopharmaceutical and physicochemical drug properties suitable for orally disintegrating tablets. ADMET and DMPK. 2016;4(4):335-360.
Available:https://doi.org/10.5599/admet.4.4.338
51. Avdeef A, Fuguet E, Llinàs A, Ràfols C, Bosch E, Völgyi G, alEquilibrium solubility measurement of ionizable drugs–consensus recommendations for improving data quality. Admet and Dmpk. 2016;4(2):117-178.
Available:https://doi.org/10.5599/admet.4.2.292
52. Yan C, Wu XY, Luo OY, Su L, Ding YT, Jiang Y, Yu DC. Diisopropylamine dichloroacetate alleviates liver fibrosis through inhibiting activation and proliferation of hepatic stellate cells. Int J Clin Exp Med. 2019;12(4):3440-3448.

Peer-review history:
The peer review history for this paper can be accessed here:
https://www.sdiarticle5.com/review-history/127798